2015 International Nuclear Atlantic Conference - INAC 2015
São Paulo, SP, Brazil, October 4-9, 2015
ASSOCIAÇÃO BRASILEIRA DE ENERGIA NUCLEAR - ABEN
ISBN: 978-85-99141-06-9

NEUTRON FLUX DISTRIBUTION INSIDE THE CILINDRICAL CORE OF MINOR EXCESS OF REACTIVITY IN THE IPEN/MB-01 REACTOR AND COMPARISON WITH CITATION CODE AND MCNP-5 CODE.

Vitor O. G. Arêdes[1], Ulysses d´Utra Bitelli[1], Luiz E. C. Mura[1], Diogo F. dos Santos[1], Ana Cecília de Souza Lima[1]

[1] Instituto de Pesquisas Energéticas e Nucleares (IPEN / CNEN - SP)
Av. Professor Lineu Prestes 2242
05508-00 São Paulo, SP
ubitelli@ipen.br,

ABSTRACT

This study aims to determine the distribution of thermal neutron flux in the IPEN/MB-01 nuclear reactor core assembled with cylindrical core configuration of minor excess of reactivity with 568 fuel rods (28 fuel rods in diameter).
The thermal neutron flux at the positions of irradiation derive from the method of reaction rate using gold foils. The experiment consists in inserting gold activations foils with and without cadmium coverage (cadmium boxes with 0.0502 cm thickness) in several positions throughout the active core. After irradiation, activity induced by nuclear reaction rates over gold foils is assessed by gamma ray spectrometry using a high-purity germanium (HPGe) detector. Experimental results are compared to those derived from calculations performed using a three-dimensional CITATION diffusion code and MCNP-5 code and a proper nuclear data library. While calculated neutron flux data shows good agreement with experimental values in regions with little disturbance in the neutron flux, also showing that in the region of the reflectors of neutrons and near the control rods, the diffusion theory is not very precise.
The average value of thermal neutron flux obtained experimentally compared to the calculated value by CITATION code and MCNP-5 code respectively show a difference of 1.18% and 0.84% at a nuclear power level of 74.65 ± 3.28 % watts. The average measured value of thermal neutron flux is 4.10 10^8 ± 5.25% n/cm²s.

INTRODUCTION

Aiming to collaborate with the scientific community and studies in reactors physics, this work presents results of neutron flux of a new cylindrical configuration of the IPEN/MB-01 with a smaller excess reactivity. The choice of this configuration was made for the fact that this condition provides an almost complete withdrawal of control rods due to low excess reactivity. Thus, the neutron flux would occur in a region away from disturbance caused by control rods.

From procurement of cylindrical configuration desired, approximately 279 pcm, eight times smaller than the default 28x26 rectangular, the neutron field was characterized by measuring the spatial distributions [1].
The values of thermal neutron were obtained experimentally by irradiating bare gold foil and covered with cadmium and measure the nuclear reaction rate of radioactive induced in these activation detectors irradiated in a certain position in the reactor core.

2015 International Nuclear Atlantic Conference - INAC 2015
São Paulo, SP, Brazil, October 4-9, 2015
ASSOCIAÇÃO BRASILEIRA DE ENERGIA NUCLEAR - ABEN
ISBN: **978-85-99141-06-9**

The objective of this work is to obtain experimental values of the curvature of the neutron flux in the axial direction, radial north-south and radial east-west, into the asymptotic region of the reactor core in its cylindrical core configuration, away from the disturbances caused by reflector and control bar and compare to the calculations performed with the three-dimensional CITATION diffusion code using an appropriated nuclear data library.

METHODOLOGY

2.1 Experimental data.

The cylindrical configuration of lower excess of reactivity found by removal of fuel rods, in order to reduce the diameter of the reactor core, has a diameter of 28 fuel rods, Figure 1. The excess of reactivity of this new configuration calculated is approximately eight (8) times smaller than the default 28x26 rectangular, approximately 2457 pcm for standard configuration, and approximately 279 pcm for the new cylindrical configuration [2].

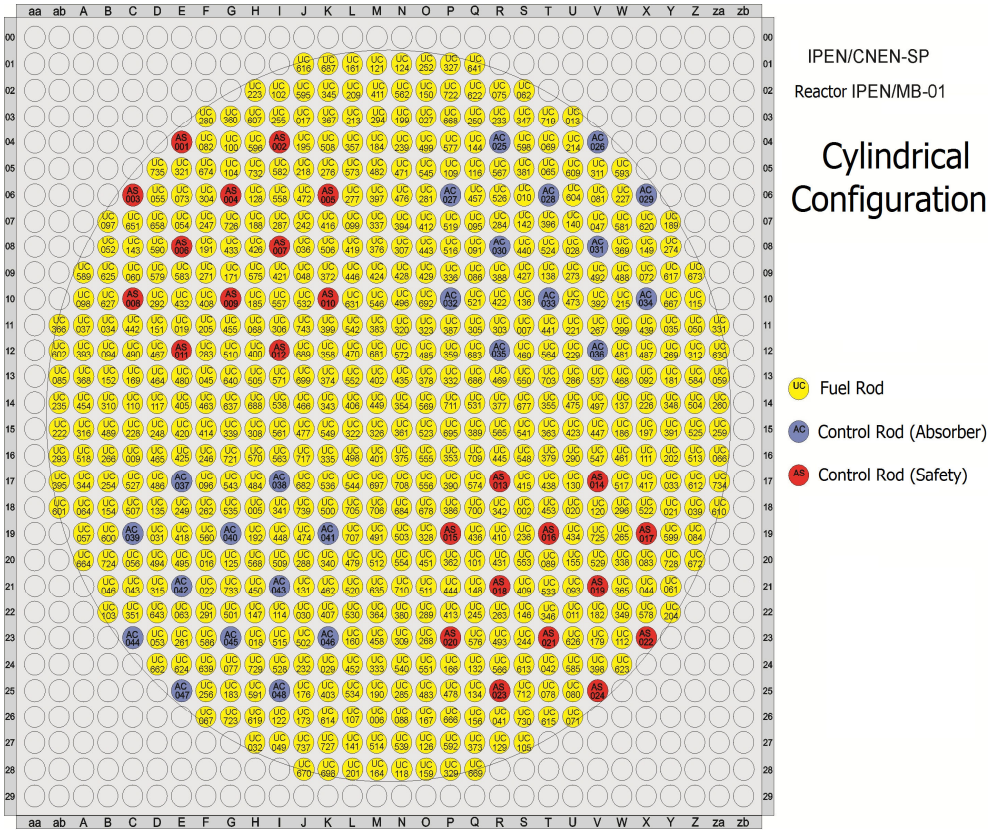

Figure 1: Cilíndrical configuration of minor excess of reactivity in the IPEN/MB-01 reactor.

For the experiments irradiation and counting of foils, we used activation foils infinitely dilute of gold-aluminum (Au-Al), with a percentage of gold in the alloy of 1.0%, which makes it unnecessary the self-shielding adjust of the neutron flux. Table 1 and 2 shows the characteristics of the activation foils.

2015 International Nuclear Atlantic Conference - INAC 2015
São Paulo, SP, Brazil, October 4-9, 2015
ASSOCIAÇÃO BRASILEIRA DE ENERGIA NUCLEAR - ABEN
ISBN: 978-85-99141-06-9

Table 1: Characteristics of the activation foils (detectors).

Irradiated foil	Nuclear reaction/ Product	Half-life of Product	Mass (g)	Thickness (cm)	Irradiation time
1%Au-99%Al *	$^{197}Au(n,\gamma)^{198}Au$	64.56 h	0.025	0.02	1 h
1%Au-99%Al	$^{197}Au(n,\gamma)^{198}Au$	64.56 h	0.025	0.02	1 h

* Coverage of cadmium 0,5 mm thick.

Table 2: Nuclear Reactions and response range of the thermal activation detectors.

Foil	Nuclear Reaction	Action Range (Mev) [b]
Au	$^{197}Au\ (n, \gamma)^{198}Au$	$1.0\ 10^{-8}$___$6.3\ 10^{-6}$
Au [a]	$^{197}Au\ (n, \gamma)^{198}Au$	$2.8\ 10^{-6}$___$3.0\ 10^{-5}$

[a] Coverage of cadmium of 0,508 mm thickness; [b] 90% of Nuclear reaction rate.

The activation foils are fixed to a board of lucite, Figure 2, inserted between the channels (spaces between the fuel rods) in the center of the reactor core. The irradiation time was estimated by the half-life of the radionuclide formed in the nuclear reaction of interest and the activation cross section of the target irradiated. In some cases the foils used were covered with cadmium aiming to avoid interference from thermal neutrons.

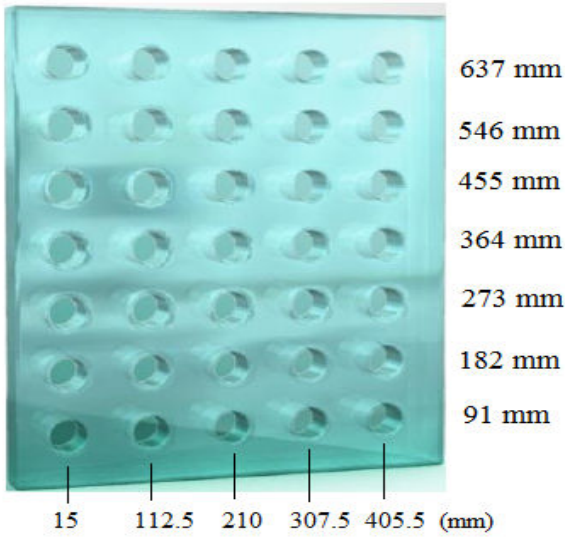

Figure 2: Illustration of lucite board and the fittings for activation detector.

The integrals counts of gamma photopic of the radionuclide were performed by a high purity germanium detector, using the MAESTRO software installed on a computer (PC). Using the ORIGIN, exponential adjustments were made from three decay counts of 20mins for each position and various counts in the central region of the core (statistically better), so as to obtain the activity value at the end of irradiation (A_0), as shown in Figure 3, and thereby its saturation activity (nuclear reaction rate at the place of irradiation).

2015 International Nuclear Atlantic Conference - INAC 2015
São Paulo, SP, Brazil, October 4-9, 2015
ASSOCIAÇÃO BRASILEIRA DE ENERGIA NUCLEAR - ABEN
***ISBN:* 978-85-99141-06-9**

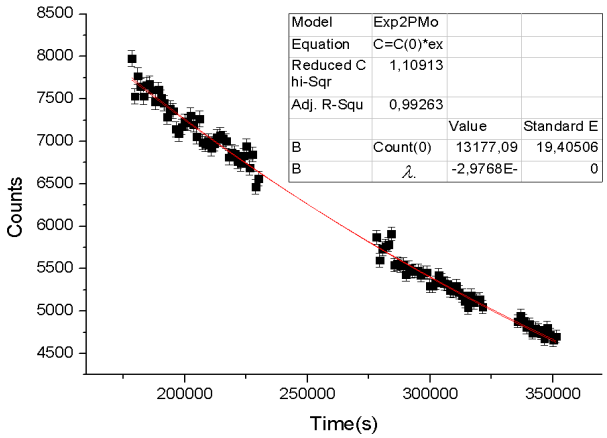

Figure 3: Exponential adjustment decay curve of the photopeak counts for the central position of the reactor core.

2.2 Monte Carlo method / MCNP-5 code

In this paper we use the computer code "Monte Carlo N Particles" (MCNP) in version 5, to solve problems through the Monte Carlo method. In this code it is possible to modeling the geometry of the problem in question, for example, a reactor core, and calculate the quantities of interest Reactor Physics. For modeling, the code works with various geometries as planes, cylinders, spheres, etc. used to build the problem in question. Together with the geometric part it is necessary to include materials that fulfill those geometries using nuclear data libraries [3,4].

In this study, the method was used for comparison and validation of calculations of the results obtained experimentally [5].

The neutron flux results were normalized by the power 74,65W [6] by equation (1) [7],

$$\overline{\Phi}_N\left[\frac{neutrons}{cm^2.s}\right]=\frac{P[w].\overline{\nu}\left[\frac{neutrons}{fission}\right]}{1{,}60217657.10^{-13}\left(\frac{Ws}{MeV}\right)\overline{Q}\left[\frac{MeV}{fission}\right].K_{eff}}.\overline{\Phi}_j\left[\frac{1}{cm^2}\right], \quad (1)$$

where ν is the average number of neutrons per fission, Φ_j is the average neutron flux in the energy interval in units of MCNP and K_{eff} is the multiplication factor K effective estimated by MCNP. The energy liberated by fission average Q and the average number of neutrons ν, was calculated in MCNP.

The F_{cd} cadmium factor used in this study was calculated by MCNP-5 using the nuclear data library ENDF/B-VI and applying equation [8] (2) below,

$$F_{cd}=\frac{R_{ep}^{\infty}}{R_{cd}^{\infty}}, \quad (2)$$

ISBN: 978-85-99141-06-9

where R_{ep} is the reaction rate of neutrons above the energy junction between the thermal spectrum and intermediate (E_j) in a bare detector and R_{cd} is the reaction rate of a detector covered with cadmium(E_{cd}).

The result obtained by MCNP-5 for cadmium factor was $F_{cd} = 1.06 \pm 2.9\%$

2.3 CITATION code

The CITATION solves equaçãoo diffusion expressing an approach to the transport of neutrons in a re energy position *E*. É descrita aqui a equação (3) no modelo de multi-grupo [9] que é usada para obter um tipo da diferença finita de contrapeso do nêutron sobre elementos discretos do volume. The equation (3) in multigroup model [9] is used to obtain one type of finite difference of the neutron balance of discrete volume elements.

$$-D_{r,g}\nabla^2\Phi_{r,g}+\left(\Sigma_{a,r,g}+\sum_n \Sigma_{s,r,g\to n}+D_{r,g}B^2{}_g\right)\Phi_{r,g}=\sum_n\left(\Sigma_{s,r,n\to g}+\frac{S_g(\upsilon\Sigma)_{f,r,n}}{K_e}\right)\Phi_{r,n}, \qquad (3)$$

where, ∇^2 is the geometric operator Laplacian, $\frac{\partial^2}{\partial x^2}+\frac{\partial^2}{\partial y^2}+\frac{\partial^2}{\partial z^2}$ in rectangular geometry in cm^{-2} , $\Phi_{r,g}$ It is the neutron flux in a position *r* and a group of energy *g* in n/s.cm², $\Sigma_{a,r,g}$ is the macroscopic cross section absorption, usually measured by a spectrum representative of the flux energy in cm^{-1}, $\Sigma_{s,r,g\to n}$ is the macroscopic scattering cross section of neutrons from the energy group *g* to the energy group *n* in cm^{-1}, $D_{r,g}$ is diffusion coefficient in cm^{-1}, $\upsilon\Sigma_{f,r,g}$ is the macroscopic cross section for the production of neutrons where υ is the number of neutrons produced by fission and Σ_f is a macroscopic fission cross section in cm^{-1}, S_g is the number of neutrons emitted per cm^3/s by the source and k_e the effective multiplication factor, the ratio between the production rate and the rate of neutrons leakage.

The calculation method used was based on Hammer-TECHNION [10] for the generation of cross sections. Then the code CITATION [11], based on neutron diffusion theory was used to calculate neutron flux distribution in three-dimensional geometry (x, y, z) for four energy groups, 10MeV, 1,05MeV, 9,12keV and 0,625eV. The center lines were chosen in the radial and axial positions.

3. THEORY

Neutrons have no electrical charge, so they are detected indirectly [12]. The technique of activation analysis is frequently used to detect them. For this work, were used detectors called activation foils composed of 1% of gold (*Au*) and 99% of aluminum (*Al*), called infinitely diluted foil [13].

The reaction that occurs at Au because of the neutronic field is radioactive capture, ^{197}Au (n, γ) ^{198}Au, the target nucleus captures a neutron and emits a gamma ray of approximately 411.80 keV with a high probability emission of 95.56%. The activation foils were irradiated in a reactor critical, but until achieve the desired power the foils are irradiated by neutronic

ISBN: 978-85-99141-06-9

field. Thus, it is necessary to correct this addition of activity due to the rise of the ramp of power, it is of interest only the activity induced in the foils because of the neutron flux for stable power [13]. The ramp factor F_R can be determined by equation (4),

$$F_R = \frac{1}{1+\frac{T}{t}} \quad . \tag{4}$$

The period T is given by equation (5),

$$T = \frac{T_R}{\ln\left(\frac{P}{P_0}\right)} \, , \tag{5}$$

where P is the final power of irradiation, P_0 is the initial power and T_R the time of ramp rise, timed from P_0 to P, as illustrated in Figure 4.

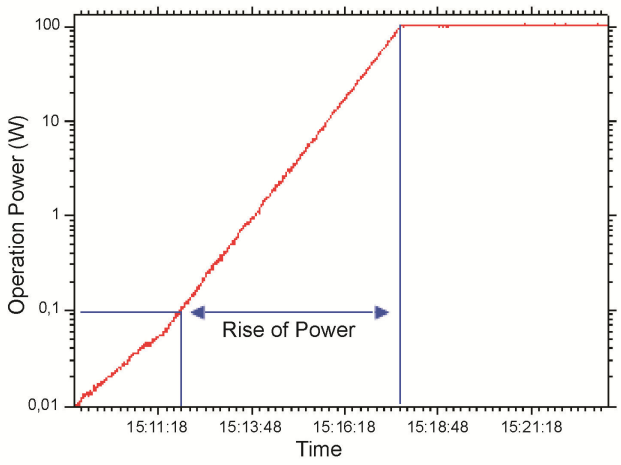

Figure 4: The power level as a function of time.

After irradiation of activation foils, waited a few minutes to decay 95% of the main fission products then these leaves were analyzed through an Ortec HPGe detector centered at the photopeak of energy 411.80 keV for the gold *(Au)*. Thus were obtained the photopic areas that are counts (net) as disintegrations per second.

The nuclear reaction rate is equal to the saturation activity which can be obtained when a detector is irradiated for an infinite time, much longer than its half-life, making impracticable the achievement of experimental saturation activity. Even if the activation foils were irradiated for a very long time, it would be impossible to take them immediately to the HPGe detector [12]. The activity of saturation on the basis of counts obtained in the detector is given by equation (6).

$$A^{\infty} = \frac{\lambda \, . \, net \, . \, e^{\lambda t_e}}{\varepsilon \, . \, I \, . \left(1 - e^{-\lambda t_i}\right) . \left(1 - e^{-\lambda t_c}\right)} = \frac{\lambda \, . \, A_0}{\varepsilon \, . \, I \, . \left(1 - e^{-\lambda t_i}\right) . \left(1 - e^{-\lambda t_c}\right)} \, , \tag{6}$$

ISBN: 978-85-99141-06-9

where, λ is the decay constant of the radioisotope formed, *net* is the photopeak area or count, A_0 is the initial activity, *te* is the waiting time between the end of irradiation and counting, *ti* is the irradiation time, *tc* is the counting time, *I* is the Branching rate and ε is the efficiency counting (HPGe).

The efficiencies ε of the HPGe detector were determined by counts of radioactive source of ^{152}Eu that had an initial activity on 01/03/1991 A_0=13.30 ± 0.29 KBq with a statistical confidence of 2σ. The counting efficiency is given by equation (7),

$$\varepsilon = \frac{net}{LT \,.\, I \,.\, A} \quad , \tag{7}$$

where, *LT* (Live Time) is the counting time discounting the "dead time" of the detector and *A* is the activity of ^{152}Eu at the time of counting.

With only two counts is possible to determine the decay curve of each position and get its initial activity A_0 by equation (8) and its activity Saturation A^{∞} (6) as shown in the Figure 5. In this case more counts improve the adjustment in the decay curve and closer to the physical reality will be the value obtained for A_0,

$$A = A_0 \,.\, e^{-\lambda \,.\, t_e} \quad . \tag{8}$$

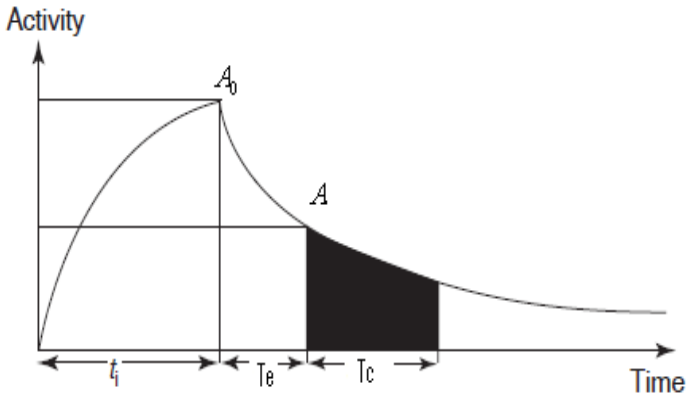

Figure 5: Variation of the activity of the detector as a function of time.

The activation detector is not only sensitive to a specific range of the neutronic spectrum. Thus, is necessary to discriminate the parcel of the the neutron energy of interest. The induced saturation activity (A^{∞}_{bare}) in bare gold foil is due to thermal neutrons and intermediates, equation (9), the parcel of fast neutrons is insignificant because of their low cross-section for energies above 1.05 MeV.

$$A^{\infty}_{bare} = A^{\infty}_{th} + A^{\infty}_{\text{int}} \quad . \tag{9}$$

For the amount related the saturation activity of intermediate flux in a foil is necessary to cover it with a small box of cadmium. Cadmium (Cd) is not a perfect filter because it does not absorbs only thermal neutrons but also intermediate neutrons and the cadmium factor fix this problem, equation (10).

ISBN: 978-85-99141-06-9

$$A^{\infty}_{\text{int}} = F_{cd} . A^{\infty}_{cd} \quad . \tag{10}$$

This factor is tabulated in literature and depends on the thickness of cadmium and the material, or may be obtained by the Monte Carlo method, equation (2).

The ratio of cadmium to the point where it is performing the measurement for infinitely diluted foil is given by equation (11).

$$R_{cd} = \frac{A^{\infty}_{bare}}{A^{\infty}_{cd}} \quad . \tag{11}$$

Thus, the thermal saturation activity can be obtained by equation (9) or (12).

$$A^{\infty}_{th} = A^{\infty}_{bare} . \left(1 - \frac{F_{cd}}{R_{cd}}\right) . \tag{12}$$

$A^{\infty} = \Sigma_{act} V \varphi$ where Σ_{act} is the average activation macroscopic cross section and V the volume of the detector. The thermal neutron flux is given by equation (13).

$$\Phi_{th} = \frac{A^{\infty}_{th} . P_a}{N_a . m . \sigma_{atv} . G_{ter}} \quad , \tag{13}$$

where, P_a is the atomic weight of the target nucleus, N_a is the Avogadro's number, m is the mass of the activation detector, σ_{atv} is the average microscopic cross section and G_{ter} disturbance factor in the thermal flux, which is canceled by the use of infinitely diluted detectors.

4. RESULTS

The efficiency found for the HPGe detector in the position used for all counts of decay in the MAESTRO software was 0.009174 or 0.9174% with an error of 0.0002 or 0.0218%. The gamma branching rate of the ^{198}Au used was 0.9556.

The cadmium factor (F_{cd}) used was calculated using the MCNP software and equation 2, it is 1.054 with an error of 2.0%.

Now will be presented results for the thermal neutron flux measured experimentally and calculated by MCNP5 code and code CITATION, in the central regions in the cylindrical configuration of the reactor core IPEN/MB-01 28x28. The flux obtained from the MCNP code in relative units were processed in real flux (n / cm².s) by multiplying the conversion factor in equation (1), calculated by the average experimental neutron flux calculated by Silva (2014) [6] and the average neutron flux calculated by MCNP-5.

Table 3 shows the comparison between the measured experimentally thermal flux and calculated by MCNP-5 and CITATION code. The radial dimensions A, B, C, D and E correspond to 15mm, 112mm, 210mm, 307mm and 405mm respectively.

ISBN: 978-85-99141-06-9

Table 3: Comparison of calculated and measured thermal flux in the irradiation channel 14-15 at a power level of 74.64 ± 2.43W.

Position	Flux Th ± (%)[a]	MCNP ± (%)[a]	CITATION
637A	1.91 10^8 ± 7.94	2.0659 10^8 ± 1.28	1.56 10^8
637B	3.10 108 ± 8.38	3.0660 108 ± 1.28	2.52 108
637C	4.79 10^8 ± 7.13	5.0048 10^8 ± 1.28	2.88 10^8
637D	4.03 10^8 ± 6.37	3.9096 10^8 ± 1.28	2.36 10^8
637E	3.66 10^8 ± 7.66	2.0519 10^8 ± 1.28	1.50 10^8
546A	1.59 10^8 ± 12.72	4.3639 10^8 ± 1.28	2.39 10^8
546B	5.73 10^8 ± 8.58	5.7929 10^8 ± 1.28	3.95 10^8
546C	8.02 10^8 ± 8.67	7.9662 10^8 ± 1.28	4.48 10^8
546D	8.16 10^8 ± 7.24	6.0361 10^8 ± 1.28	3.74 10^8
546E	5.89 10^8 ± 6.6	4.4065 10^8 ± 1.28	2.31 10^8
455A	2.30 10^8 ± 14.43	2.4515 10^8 ± 1.28	3.95 10^8
455B	7.28 10^8 ± 8.81	7.3974 10^8 ± 1.28	6.56 10^8
455C	1.05 10^9 ± 7.93	1.1460 10^9 ± 1.28	7.44 10^8
455D	1.15 10^9 ± 7.29	8.081 10^8 ± 1.28	6.26 10^8
455E	8.32 10^8 ± 6.08	3.1439 10^8 ± 1.28	3.85 10^8
364A	2.61 10^8 ± 14.88	3.2851 10^8 ± 1.28	4.86 10^8
364C	1.13 10^9 ± 7.95	1.1105 10^9 ± 1.28	9.16 10^8
364D	1.04 10^9 ± 8.41	1.0199 10^9 ± 1.28	8.11 108
364E	8.89 108 ± 6.04	3.6904 108 ± 1.28	4.82. 10^8
273A	2.37 10^8 ± 13.24	3.5983 10^8 ± 1.28	5.36.10^8
273B	7.39 10^8 ± 8.34	8.3205 10^8 ± 1.28	9.05 10^8
273C	1.08 10^9 ± 8.19	1.1434 10^9 ± 1.28	1.01 10^9
273D	1.08 10^9 ± 7.82	9.9577 10^8 ± 1.28	9.04 10^8
273E	7.26 10^8 ± 7.19	3.9980 10^8 ± 1.28	5.35 10^8
182A	2.02 10^8 ± 13.18	2.0711 10^8 ± 1.28	3.76 10^8
182B	5.27 10^8 ± 8.73	5.5835 10^8 ± 1.28	6.34 10^8
182C	7.88 10^8 ± 8.25	7.7131 10^8 ± 1.28	7.09 10^8
182D	7.56 10^8 ± 7.21	5.4625 10^8 ± 1.28	6.34 10^8
182E	5.44 10^8 ± 6.07	2.3276 10^8 ± 1.28	3.76 10^8
91A	1.94 10^8 ± 8.39	2.0890 10^8 ± 1.28	2.61 10^8
91B	3.55 10^8 ± 7.11	3.3476 10^8 ± 1.28	4.33 10^8
91C	4.99 10^8 ± 8.72	5.2660 10^8 ± 1.28	4.87 10^8
91D	5.19 10^8 ± 6.78	3.7582 10^8 ± 1.28	4.33 10^8
91E	3.76 10^8 ± 6.71	2.9907 10^8 ± 1.28	2.61 10^8

[a] Uncertainties (%) at the level of statistical confidence 2σ.

ISBN: 978-85-99141-06-9

Despite the small discrepancy between the punctual flux values measured and calculated, both methods CITATION, MCNP and experimental presents the average flux very concordant, discrepant only about 1%, according to Table 4.

Table 4: Comparison between the average thermal neutron fluxes calculated by CITATION and MCNP-5 and measured experimentally.

Energy range (eV)	CITATION [a] (n/cm².s)	MCNP-5 (n/cm².s)	Experimental (n/cm².s)
$\Phi < 0.55$	$4.1008\ 10^{8}$	$4.0188\ 10^{8}\pm1.2\%$	$4.0529\ 10^{8}\pm3.27\%$

[a] $\Phi<0.625$ eV

The average calculated by CITATION (deterministic calculation) was corrected to 74.64W, in MCNP5 we calculated the average flux in the cell of the active volume of the reactor core, the average of the experimental measurements were normalized by variance.

In Figures 6 and 7 below, show up comparisons between experimentally measured neutron flux and calculated by CITATION code [11] and MCNP-5 code, according to work presented by Bitelli and Lima [14]. Uncertainties associated with at 95% and statistical confidence level of 2σ.

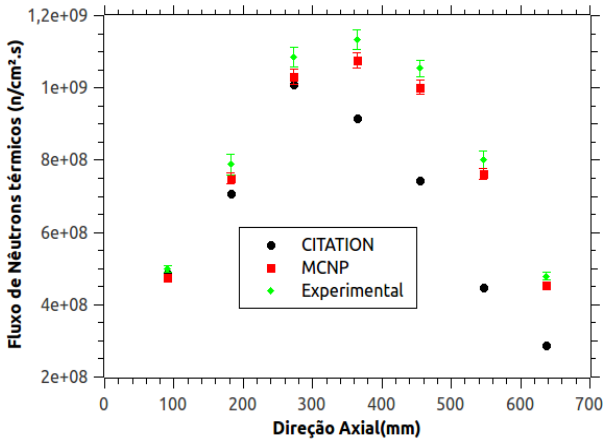

Figure 6: Comparison between measured and calculated thermal neutron flux in the axial region.

ISBN: **978-85-99141-06-9**

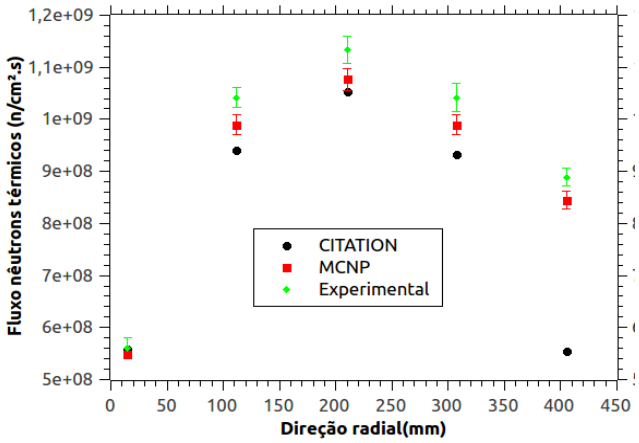

Figure 7: Comparison between measured and calculated thermal neutron flux. in the east-west radial region.

5. CONCLUSIONS

The values found for the neutron flux met expectations, since the higher flux values are located in the center of the reactor core.

The minor excess of reactivity of this cylindrical configuration decreased the disturbance caused by the control rods in the values of neutron flux. The control rods were almost completely removed, and the values for the neutron flux in the upper part of the reactor core approached to the value of the bottom, away from disturbance of control rods, according to Table 3.

When comparing the average values of thermal neutron flux measured experimentally and calculated by CITATION and MCNP-5 respectively, we find a discrepancy of only 1.18% and 0.84%, absolutely within the ranges of uncertainty experimental values. The punctual values calculated by the MCNP were closer to the experimental values of flux and varying by 2% with experimentally measured average flux values. Therefore we can say that CITATION is an excellent program to obtain integral values as the integral neutrons flux in the core or the average flux.

As a proposal for further work, we suggest obtaining the distribution of neutron flux with other types of activation detectors, thermal and epithermal, and a full mapping using activation wires that will provide a more complete and better view of the flux distribution.

ACKNOWLEDGMENTS

The results obtained in this paper had the participation of the colleagues Cesar Luiz Veneziani, Hugo Rodrigues Landim and the manager of the IPEN/MB-01 reactor Mr. Rogério Jerez by changing the core configuration and operation of the reactor IPEN/MB-01.

ISBN: **978-85-99141-06-9**

REFERENCES

1. Zjolnay.E.M. "Neutron Flux and Spectrum Measurement by Activation Method". *Lectures Notes for the Training Course and Measurements of Neutron Flux Spectrum for Research Reactor IAEA.* Indonesia. Hacarta. 27 september-15 October.1993.

2. AREDES. O. G. V. "Caracterização Do Núcleo Cilíndrico De Menor Excesso De Reatividade Do Reator Ipen/Mb-01. Pela Medida Da Distribuição Espacial E Energética Do Fluxo De Nêutrons". São Paulo: 2014. Dissertação de Mestrado- Instituto De Pesquisas Energéticas E Nucleares.

3. HARMON. C.D.. BUSCH. R.D.. BRIESMEISTER. J.F.. FORSTER. R.A. **"**Criticality calculations with MCNP: A Primer". *Los Alamos National Laboratory*. LA-12827-M Manual. 1994.

4. RIEMEISTER. J.F. MCNP: *A General Monte Carlo N-Particle Transport Code (Version - 4C)*. Los Alamos National Laboratory. LA-13709-M. 2000.

5. ISLARNABAD. P. O. N. "Comparison of Experimental and calculated neutron spectra for pakistain reseach reactor-1". Nuclear Engeneering Division Pakistan Institute of Nuclear Science and Tecnology. Pakistan 1995.

6. SILVA. A. P. "Cálculo Da Potência Do Reator Ipen/Mb-01 No Formato Cilíndrico 28x28 Varetas Combustiveis De Menor Excesso De Reatividade". São Paulo: 2014. Dissertação De Mestrado- Instituto De Pesquisas Energéticas E Nucleares.

7. Luka Snoj. Matjaž Ravnik. "Calculation of Power Density with MCNP in TRIGA reactor". International Conference Nuclear Energy for New Europe 2006 . Portorož. Slovenia. September 18-21. 2006.

8. Beckurtz. K.H.;Wirtz. K. Neutron physics**.** New York. Springer. 1964.

9. LAMARSH. J.R. "Introduction to nuclear reactor theory". Addison-Wesley Publishing Company. 1972.

10. BARHEN. J.; RHOTENSTEIN. W. and TAVIV. E.. "The HAMMER Code System Technion". Israel Institute of Technology. Haifa. Israel. NP-565. 1978.

11. Fowler.T.B.; Vondy. D.R.; Cunningham. G.W.. "Nuclear Reactor Core Analysis Code: CITATION". Oak Ridge National Laboratory. ORNL-TM-2496. Revision2. July.1971.

12. Bench. F. ; Fleck.C.M. "Prática de Física de Nêutrons" - **Volume 2**. pág.306. Tradução DERE/IEN.

13. RANT. J. *Measurements of neutron flux distributions by activation detectors***.** In: *International Atomic Energy Agency*. Aplication of small computers to research reactor operation: international training course. Ljubljana. 1-26 Jun.. 1987.

14. LIMA. A.C.S.; BITELLI. U.d'U. *Cálculo da Distribuição de Fluxo de Neutrons no Nucleo Cilindrico de 28x28 do Reator IPEN/MB-01*. Relatorio P&D.CENR.069.00. abril. 2014.